Article

Memory and Spectral Diffusion in Single-Molecule Emission

Kristin L. Wustholz, Eric D. Bott, Bart Kahr, and Philip J. Reid

J. Phys. Chem. C, **2008**, 112 (21), 7877-7885 • DOI: 10.1021/jp711687j • Publication Date (Web): 10 April 2008

Memory and Spectral Diffusion in Single-Molecule Emission†

Kristin L. Wustholz, Eric D. Bott, Bart Kahr,* and Philip J. Reid*

Department of Chemistry, University of Washington, Box 351700, Seattle, Washington 98195-1700

Received: December 12, 2007; Revised Manuscript Received: January 15, 2008

The blinking dynamics of single violamine R (VR) molecules embedded in crystals of potassium acid phthalate (KAP) are analyzed using threshold and change-point detection (CPD) methods (Watkins, L. P.; Yang, H. *J. Phys. Chem. B* **2005**, *109*, 617). Analysis employing thresholding resulted in power-law distributions of on and off times corresponding to a power-law exponent of ~2, consistent with a distributed kinetics model for population and depopulation of the nonemissive state. When the same emission time traces were analyzed using the CPD method, a power-law exponent of ~1.5 is obtained. In addition, multiple emission states are observed using CPD, inconsistent with a simple two-state blinking model, and indicative of spectral diffusion. The role of spectral diffusion in the distributed blinking kinetics of KAP/VR is investigated by spectrally decomposing the emission using a dichroic mirror. Combining the CPD method with this experiment yielded the emission energy, intensity, and temporal duration of blinking events. A wide distribution of emission energies is observed, consistent with molecules experiencing a variety of dielectric environments within the crystal host. Time-dependent fluctuations in the spectral decomposition are observed, corresponding to spectral diffusion. Blinking events exhibited by single VR molecules in KAP are correlated, an effect referred to as memory. To our knowledge, this is the first reported observation of memory for a molecular system. Positive correlations are observed for consecutive on times and consecutive off times. In addition, adjacent on and off times demonstrate anticorrelation. These observations support the observation of spectral diffusion in this crystal environment, with this diffusion contributing to population and depopulation of the nonemissive state.

Introduction

Single-molecule spectroscopy (SMS) allows for photophysical measurements of individual luminophores revealing behavior undetectable in ensemble measurements. A familiar example of the insight provided by SMS is the emission from an individual molecule under continuous excitation. This emission is often intermittent, consisting of emissive and nonemissive periods, a phenomenon referred to as "blinking". Commonly, blinking is attributed to nonradiative transitions between optically bright and dark vibronic states (e.g., the first excited singlet and triplet states). In this case, the on-time and off-time durations can be assembled into histograms and modeled using exponential functions to extract the rate constant for decay of the optically bright singlet state (e.g., intersystem crossing), and decay of the optically dark triplet state (e.g., internal conversion to the ground state).[1–4]

Recent studies have found that a variety of chemical systems demonstrate complex blinking behavior that is inconsistent with population relaxation occurring with well-defined rate constants.[5–17]Specifically, the on- and off-time histograms for rhodamine 6G in poly(vinyl alcohol),[16] and on glass,[10] perylene diimide molecules in PMMA,[6] as well as the dye Atto565 on glass[14] are reproduced by a power-law function of the form $P_{on/off} \propto t^{-m}$ where m is the power-law exponent. The observation of power-law behavior is consistent with a distributed kinetic process in which the population/depopulation rate constants are not single valued, but instead vary with time. In particular, the rate constants for population and depopulation of the nonemissive state have been described as $k_{ij} = \kappa_{ij}e^{-x}$, where i and j are the initial and final states, respectively, κ_{ij} is the pre-exponential factor, and x is a time-dependent variable.[8,13] Etiologies offered to account for distributed kinetics for single molecules include molecular rotation,[18] conformational flexibility,[9,12] spectral diffusion,[13,19–22] reversible photo-oxidation,[23,24] and intermolecular electron transfer.[5,7,10,11,14,16] However, ambiguity remains regarding the nature of the dark state and the underlying dynamics that provide for distributed kinetic behavior.

We previously demonstrated the use of simple crystals as hosts of complex luminophores for the study of single-molecule photophysics in well-defined environments (e.g., Figure 1).[13,25] For example, individual violamine R (VR) fluorophores embedded in crystals of potassium acid phthalate (KAP) were found to exhibit blinking dynamics consistent with power-law behavior ($m \sim 2$ for both the on-time and off-time distributions).[13] This behavior was reproduced using a distributed kinetics model for population and depopulation of the nonemissive state.[8,13] Two possible mechanisms for distributed kinetics in KAP/VR were proposed: (1) time-dependent geometrical changes in the first-coordination sphere of a fixed molecule (i.e., dynamical spectral diffusion) and (2) dynamic environmental and/or conformational heterogeneity in combination with charge separation and recombination. In the first hypothesis, configurational changes modify the arrangement of the molecule relative to the surrounding dielectric, thereby altering the overlap between the molecular absorption band and the exciting field. The second hypothesis has been proposed for other molecular systems in disordered environments;[5,7,10,11,14,16,17] however, the absence of correlation between blinking dynamics and molecular orientation suggests that intermolecular charge transfer is not solely responsible for the distributed kinetics observed in KAP/VR.[13]

Herein, we investigate the origin of distributed blinking kinetics in dyed crystals. First, a robust change-point analysis

† Part of the "Larry Dalton Festschrift".

* To whom correspondence should be addressed. E-mail: kahr@chem.washington.edu (B.K.); preid@chem.washington.edu (P.J.R.).

10.1021/jp711687j CCC: $40.75
Published on Web 04/10/2008

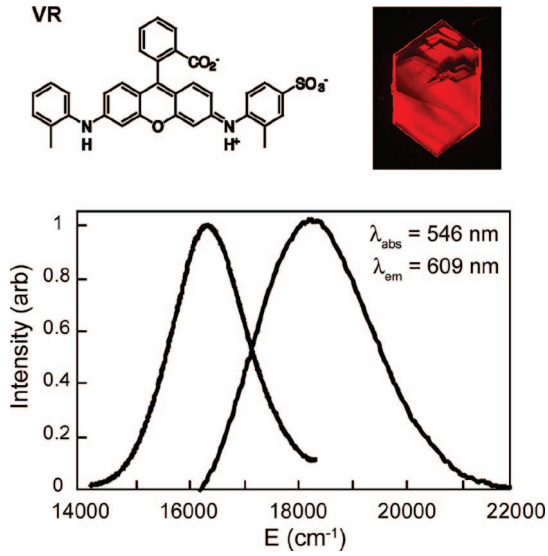

Figure 1. Ensemble-averaged absorption and emission spectra of potassium acid phthalate (KAP) crystals heavily dyed with violamine R (VR). The structure of VR is shown with a corresponding photograph of the emission from a heavily dyed crystal.

of blinking dynamics developed by Yang and co-workers is implemented in order to quantify blinking dynamics and perform a rigorous interpretation of the photophysical data.[26,27] A comparison is made of the on- and off-time probability distributions obtained by thresholding versus the change-point detection method. The role of spectral diffusion as an origin for the distributed kinetics exhibited by single molecules of VR in KAP is examined by measuring the spectral evolution of the single-molecule emission with time. Finally, correlations between adjacent on and off events (i.e., memory) in single-molecule emission are examined. Ultimately, the work presented here is consistent with complex molecular photophysics of VR in KAP involving intermolecular electron transfer, a hypothesis supported by the observations of power-law blinking behavior with $m \sim 1.5$ as well as spectral diffusion and memory effects in single-molecule emission.

Experimental Section

Heavily dyed crystals were grown as described previously.[13,25] VR (Aldrich) was dissolved in deionized water (Barnstead NANOpure, 18.2 MΩ cm^{-1}) prior to addition to the aqueous crystal-growth solution (110 g/L KAP). Single crystals of KAP/VR with chromophore densities suitable for single-molecule investigations were grown from ~5 nM dye solutions. Single-molecule studies were performed using an inverted confocal microscope described in detail elsewhere.[13,25] Dyed crystals were mounted on a scan stage (Queensgate, NPS-XY-100B) and photoexcited at low power (3.5−6.4 μW) using a 532-nm Nd:YVO_4 (Spectra Physics, Millenia) laser. The excitation field was filtered (Chroma, Z532/10-nm bandpass for 532-nm excitation), reflected toward the sample using an appropriate dichroic mirror (Chroma, Z532RDC), and focused to a diffraction-limited spot using a 100× oil-immersion objective (Nikon, PlanFluor 1.3 NA). Epi-fluorescence was collected from the sample, passed through the dichroic mirror, spectrally filtered using an emission filter (Chroma, HQ550-nm long-pass for 532-nm excitation), and spatially filtered with a confocal pinhole (CVI, 75-μm diameter). Emission was detected using a single-photon-counting avalanche photodiode (PerkinElmer, SPCM-AQR-16).

Emission traces were acquired for 100 s using a 50-ms integration time per point. From the emission traces, on and off times were initially quantified by setting an intensity threshold corresponding to the average between the mean on and off intensities (i.e., $(\langle I_{on}\rangle + \langle I_{off}\rangle)/2$) as described previously.[13] The change-point detection method is based on the algorithm developed by Yang and co-workers and was implemented in Matlab.[26,27] Consistent with previous analyses, continuous distributions of the on- and off-time probability densities ($P(\tau_{on/off})$) were derived from these data.[28]

For spectral-diffusion experiments, the single-molecule emission was separated using a dichroic mirror (Edmund Optics, NT44−266, 50%T at 600 nm) and collected with two single-photon-counting avalanche photodiodes (PerkinElmer, SPCM-AQR-16). Ensemble-averaged fluorescence measurements were corrected for monochromator and detector sensitivities of the fluorimeter (SPEX FluoroMax-2) by calibrating with a standard QTH light source. Values of the average ratio of reflected to transmitted intensity ($\langle R(t)\rangle$) corresponding to off intensities (i.e., normalized intensity = 0 and $\langle R(t)\rangle = 1$) were not included in the histogram analysis. $\langle R(t)\rangle$ values were converted to an approximate energy shift (ΔE) with respect to the emission maximum of the ensemble-averaged spectrum (i.e., 609 nm or 16 420 cm^{-1}) by convolving the transmission spectrum of the dichroic mirror with the emission of heavily dyed KAP/VR following 532-nm excitation fit to a Gaussian function. Specifically, the emission spectrum was shifted in energy at regular intervals from −5000 to +5000 cm^{-1} with respect to $\Delta E = 0$, overlaid with the transmission spectrum of the dichroic mirror, and the areas under the reflected and transmitted spectral regions were integrated in Matlab in order to obtain a functional form for $R(t)$ versus ΔE.

Correlations between adjacent on and off times were examined by analyzing $x-y$ plots on logarithmic scales consistent with previous studies.[29] The linear Pearson correlation coefficient (R_{log}) was used to quantify correlations between adjacent times:

$$R_{log} = \frac{\sum_n (x_n - \bar{x})(y_n - \bar{y})}{\sqrt{\sum_n (x_n - \bar{x})^2}\sqrt{\sum_n (y_n - \bar{y})^2}}$$

where x and y correspond to the logarithm of the on (or off) time plotted on the abscissa and ordinate, $\bar{x}$ and $\bar{y}$ are the averages of x and y, respectively, and the sums are performed over all (n) points.

Results and Discussion

Blinking Dynamics in Violamine R Dyed KAP. Heavily dyed crystals of KAP/VR demonstrate a 546-nm absorption maximum and a 609-nm fluorescence maximum (Figure 1) as measured using a microabsorption spectrometer and fluorimeter, respectively. A confocal microscope employing excitation at 532 nm ($\sigma_{KAP/VR\ (aq)}$(532 nm) = 37 500 M^{-1} cm^{-1}) was used to capture the blinking of single VR molecules embedded in KAP. Figure 2a presents an emission time trace of a representative single molecule. By visual inspection, the molecule appears to undergo transitions between two states, on and off, with corresponding intensities at roughly 80 and 40 counts per 50 ms, respectively. In our previous work, a simple threshold analysis was used to define when the molecule exists in an emissive state (Figure 2a, solid line).[13] The threshold value is defined as the average between the mean of largest and smallest intensities, and the intensity at a given time above and below the threshold value is considered to be on and off, respectively. In this framework, change points between emissive and non-

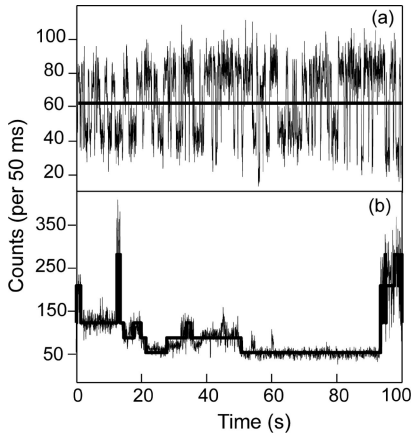

Figure 2. Emission time traces from two single molecules of VR in KAP. (a) Emission trace analyzed with a threshold (solid line) parces the trace into on- and off-time durations. (b) Emission trace analyzed with change-point detection (CPD) method developed by Yang et al. demonstrating that five statistically significant intensity levels are observed.

emissive events correspond to intensity-threshold crossings. Therefore, on (off) times are defined as the temporal duration of successive on (off) events prior to a change point. As is well-known, setting the "proper" threshold is critical to accurately quantify blinking that occurs over multiple timescales since both fast and slow blinking can be obscured by setting a threshold that is inappropriate.[26] Even more problematic is that applying a single threshold to blinking data presupposes and restricts the interpretation to two-state blinking. Therefore, we previously limited our blinking analysis to emission time traces that appeared to exhibit only two states (although multiple emission states are commonly observed). To precisely characterize blinking dynamics in dyed crystals, we implemented a robust change-point analysis of blinking dynamics.[26]

Threshold and Change-Point Detection Analyses of Blinking Dynamics. Recently, Yang and co-workers presented an algorithm for the detection of discrete change points in emission intensity traces from single emitters.[26,27] In this change-point detection (CPD) approach, statistically determined intensity change points are calculated, circumventing the problems associated with threshold analysis. In particular, spurious short-time events (e.g., shot noise, Poisson counting noise) will generate artificial change points when a threshold is used to discriminate between on and off events. Therefore, the analyzed data will contain many erroneous short-time events and correspondingly fewer events at long times. Thresholding is also problematic because it assumes knowledge of the intensity-state distribution. Placement of a single threshold is based on the assumption of a two-state system with one on and one off intensity. However, many examples exist of single emitters exhibiting more than two intensity states in blinking dynamics. To circumvent the challenges confronted when employing a threshold analysis, we implemented the CPD algorithm.[26]

In the CPD approach, the single-molecule temporal-emission traces are analyzed in a statistically unbiased and systematic fashion. Incoming photons and detector noise are modeled as Poisson distributed and intensity change points are detected through a generalized likelihood ratio test. Briefly, the probability that a change point occurred at a given time is calculated and compared to the probability of no change point. Then, change points are located at the maximum of the corresponding likelihood ratio with an uncertainty obtained by direct comparison to a type-I (false positive) error threshold. A significant advantage of the CPD approach is that the most likely number and location of intensity levels are calculated, lifting the restriction of two-state analysis. Initially, the n detected change points denote $n + 1$ unique intensity levels. These are grouped together using another likelihood ratio calculation comparing the probability of assigning any two intensity levels to a single emission state. Intensity levels are grouped iteratively until all levels have all been assigned to a single emission state. The true number of states is determined through Bayesian information criterion, which weighs the marginal information increase upon the inclusion of another emission state against the penalty of adding extra adjustable parameters. Ultimately, the CPD method reports the change-point locations as well as the number and temporal durations of intensity levels (i.e., emission states).

Blinking dynamics of single molecules in KAP/VR were analyzed with the CPD method and the results of this analysis for a representative emission time trace is shown in Figure 2b. The change points (i.e., blinking events) and five distinct deconvolved intensity levels obtained using CPD are presented. The observation of multiple emission states is consistent with spectral diffusion that is a consequence of dynamic environmental heterogeneity in the crystal (i.e., configurational changes of the dye with respect to the host). In order to generate histograms of on and off times, the emission intensity levels of each molecule were normalized. Then, the lowest normalized intensity level ($I_{\text{lowest}} < 0.3$) was defined as off, while the remaining emissive levels were defined as on. Using this analysis, the durations of on and off events were compiled into probability distributions and compared to the data obtained on 40 KAP/VR molecules using thresholding.

The on-time and off-time probability distributions for the same 40 molecules in KAP/VR obtained using CPD and thresholding are shown in Figure 3. Figure 3a demonstrates that when thresholding is used to quantify blinking dynamics both $P(\tau_{\text{on}})$ and $P(\tau_{\text{off}})$ are well described employing a power-law expression of the form $P(\tau_{\text{on/off}}) = P_0\tau_{\text{on/off}}{}^{-m_{\text{on/off}}}$ where $m_{\text{on/off}}$ is the power-law exponent. The best fits to the power-law function corresponding to $P_0(\text{on}) = 371$, $m_{\text{on}} = 2.0$, and $P_0(\text{off}) = 208$, $m_{\text{off}} = 1.8$ are presented in Figure 3, panels a and b, respectively. Blinking dynamics analyzed using the CPD method also demonstrated power-law behavior corresponding to $P_0(\text{on}) = 51$, $m_{\text{on}} = 1.1$, and $P_0(\text{off}) = 14$, $m_{\text{off}} = 1.0$. However, since the formal change-point analysis removes a substantial number of spurious (i.e., statistically insignificant) events, the number of emissive and nonemissive events is significantly reduced as compared to the thresholding analysis. Recently, a maximum likelihood estimator (MLE) method for analyzing power-law distributed data with particular application to limited data sets has been described.[30] Applying the MLE method to the total data set consisting of 40 molecules of KAP/VR analyzed with the CPD method resulted in power-law exponents of $m_{\text{on}} = 1.3$ and $m_{\text{off}} = 1.2$. When the entire distribution of event durations was compiled (i.e., events were not separated into on and off times based on normalized intensities), best fit to the power-law function corresponded to $P_0 = 110$, $m = 1.3$. For comparison, the power-law exponents observed for other systems are typically $m \sim 1.7$ for semiconductor nanocrystals,[28,31,32] $m \sim 2$ for single molecules on glass,[10,14] and $m \sim 1.5$ for molecules dispersed in polymers.[5,7] Recently, the impact of the surrounding dielectric on the power-law exponent of semiconductor quantum dots in polymers and on crystalline surfaces was investigated.[33] Power-law behavior with $m \sim 2$ was also observed for individual molecules of VR in KAP, demonstrating that the power-law dependence is not a consequence of averaging over many

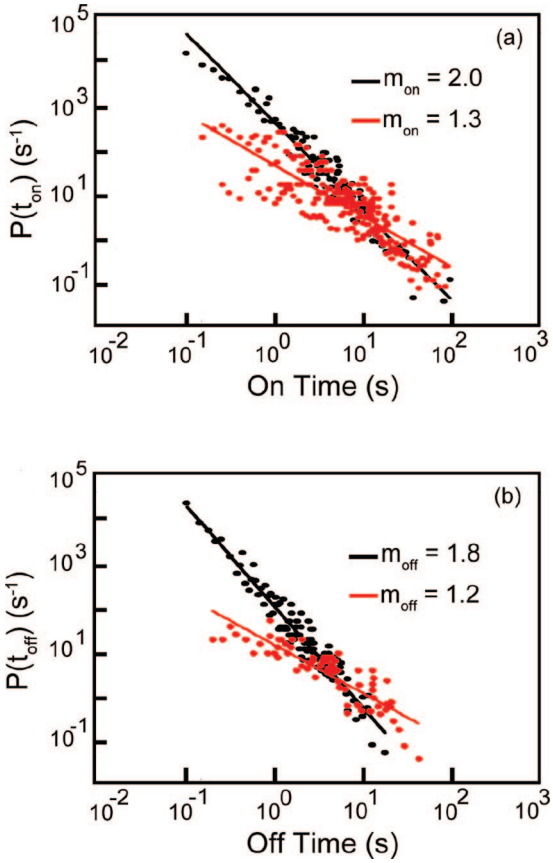

Figure 3. On- and off-time probability distributions for 40 molecules of VR in KAP. (a) On-time probability distributions for data analyzed by thresholding (black) and CPD method (red) demonstrating modification of the power-law exponent from m_{on}= 2.0 to m_{on} = 1.3 (MLE). (b) Corresponding off-time probability distributions for data analyzed by thresholding (black) and CPD method (red) demonstrating modification of the power-law exponent from m_{on}= 1.8 to m_{on} = 1.2 (MLE). As expected, the number of short-time events is significantly reduced with application of the rigorous CPD method.

molecules with distributed single-exponential rates.[13] When the same individual molecules are subjected to the CPD method, the number of blinking events is significantly reduced. Applying the MLE method to an individual molecule recorded for ~1800 s resulted in power-law exponents of m_{on} = 1.2 and m_{off} = 1.2, consistent with the exponents for the collection of molecules.

Comparing the results of threshold analysis to the CPD method demonstrates that the power-law exponents of on and off times are modified from $m \sim 2$ to ~1.5. Visual inspection of the data illustrates that the power-law exponents are reduced due to a decrease in the number of short-time events, consistent with the prediction that the CPD method removes spurious change points associated with Poissonian noise. In any case, power-law behavior is conserved over 3 orders of magnitude in time, and power-law fit to the data at long times (i.e., 1−100 s) is similar for both thresholding and CPD methods. The comparison of blinking data analyses demonstrates two significant results. First, the necessity of applying the CPD method to quantify blinking is readily evident. Spurious short-time data originating from implementation of a hard threshold artificially increased the power-law exponent. Second, with accurate treatment of blinking data, a rigorous interpretation of the nature of the nonemissive state and the origin of power-law statistics becomes possible. In our previous work we proposed that the distributed kinetics observed in KAP/VR originate from modification of the local dielectric leading to spectral diffusion and/or intermolecular electron transfer. In the first hypothesis, the orientation of the molecule relative to the surrounding dielectric is modified (e.g., a potassium ion becomes closer to the dye), thereby altering the overlap between the molecular absorption band and the exciting field. The second hypothesis has been proposed for other molecular systems;[5–7,10,11,14,16,17] however, our previous work suggested that intermolecular charge transfer is not solely responsible for the distributed kinetics observed in KAP/VR.[13] Yet, the new insight provided by the CPD algorithm, revealing power-law exponents closer to 1.5, is consistent with a blinking mechanism related to electron transfer.[34] In the following section, we explore the first hypothesis, spectral diffusion, in the blinking dynamics of single molecules in KAP/VR.

Role of Spectral Diffusion in Distributed Kinetics. Single molecules in solid hosts are known to exhibit spectral diffusion, largely due to fluctuations in the excitation rate due to spectral shifts of the absorption spectrum.[21,22,35] Correlation between a reduction in emission intensity with modified spectral position was recently observed for single molecules of DI and DAPI in polystyrene films.[21,22] The observation of multiple emission intensities (e.g., Figure 2b) has also been linked to spectral diffusion. For example, the time-dependent emission intensity from individual quantum dots can exhibit several on intensities consistent with spectral diffusion associated with electron transfer.[27,36] Given the evidence for spectral diffusion in other systems, we explored the role of spectral diffusion in the blinking dynamics of single VR molecules in KAP.

To measure spectral diffusion, we adopted a simple experimental approach that allowed us to monitor modifications to the emission energy from one molecule to another as well as the time-dependent intensity changes associated with spectral diffusion.[37] Specifically, the emission from a single molecule was separated into two spectral components with each component delivered to an avalanche photodiode using a dichroic mirror centered at 600 nm. With this simple experimental setup one detector collected transmitted light of energies between 550 and 600 nm, the other collected reflected emission >600 nm. The average of the ratio reflected to transmitted intensity then provides a measure of the single-molecule emission energy (i.e., $\langle R(t)\rangle = \langle I_{reflected}/I_{transmitted}\rangle$). For example, the ensemble-averaged emission spectrum of KAP/VR is expected to give rise to an $\langle R(t)\rangle$ of 1.3, corresponding to the ratio of integrated areas of spectral components associated with reflected and transmitted intensities for emission centered at 609 nm. Indeed, the experimentally obtained value of $\langle R(t)\rangle$ measured on heavily dyed KAP/VR crystals was 1.4, consistent with the theoretical value.

Fluctuations in single-molecule $\langle R(t)\rangle$ values from the ensemble-averaged value provide a measure of the effective dielectric heterogeneity of the crystal matrix. Moreover, time-dependent fluctuations in $\langle R(t)\rangle$ for individual molecules contain information about spectral diffusion. Since molecules in single crystals of KAP do not exhibit reorientational dynamics (i.e., molecular orientation is static),[25] spectral diffusion is not associated with orientational dynamics of single molecules as is the case in other systems.[38] Rather, it is thought that dynamic conformational changes between the first coordination sphere of the host and the dye molecule will result in modifications to the dielectric, leading to spectral diffusion. Ultimately, the advantage of this simple approach in combination with the CPD method is the determination of deconvolved emission intensity levels with corresponding durations and associated $\langle R(t)\rangle$ values. Therefore, we can explore the single-molecule distribution of $\langle R(t)\rangle$ values

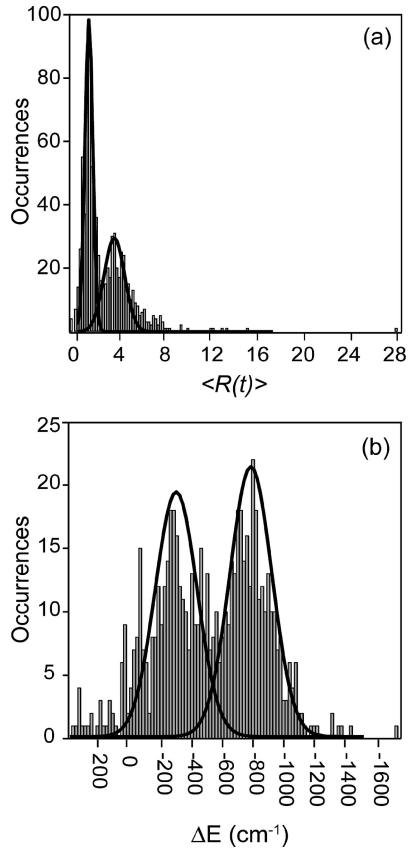

Figure 4. Histograms of (a) $\langle R(t)\rangle$ and (b) ΔE values for 61 molecules of VR in KAP corresponding to 820 events deconvolved using the CPD method. (a) Distribution of $\langle R(t)\rangle$ values exhibits two subpopulations centered at $\langle R(t)\rangle = 1.5$ and 3.8. (b) $\langle R(t)\rangle$ converted to energy shifts (ΔE) from the emission maximum of the ensemble-averaged spectrum demonstrates two red-shifted populations corresponding to emission centered at 620 and 639 nm.

(i.e., spectral shifts) as they relate to single-molecule emission intensity without presupposing two-state blinking, as well as the time-dependence of $R(t)$ for individual molecules.

The distribution of $\langle R(t)\rangle$ values was compiled for 61 molecules in KAP/VR. Analysis of the sampled molecules using the CPD method resulted in 820 emissive events with an average value for $\langle R(t)\rangle = 2.9 \pm 2.2$, where the error represents the standard deviation from the mean. The distribution of $\langle R(t)\rangle$ values best fit to two Gaussian functions centered at $\langle R(t)\rangle =$ 1.5 and 3.8 are presented in Figure 4a. Of 820 events, only 58 (7.1%) corresponded to ensemble-averaged emission (i.e., $\langle R(t)\rangle \sim 1.3$). Instead, most events (638 or 77%) exhibited comparatively large values (i.e., $\langle R(t)\rangle > 1.3$), corresponding to red-shifted emission. Values of $\langle R(t)\rangle$ were converted to energy shifts from the maximum of the ensemble-averaged emission spectrum (i.e., ΔE from 609 nm) by convolving the transmission spectrum of the dichroic mirror with the emission spectrum of heavily dyed KAP/VR. Figure 4b presents the distribution of ΔE values, with best fit to a sum of two Gaussians centered at $\Delta E = -302$ and -760 cm^{-1} corresponding to two red-shifted emission subpopulations at 16 120 (620) and 15 659 cm^{-1} (639 nm). The broad distribution of emission energies suggests that molecules experience a distribution of local dielectric environments. The single-molecule distribution of emission energies is at a variance with the ensemble-averaged spectrum of heavily dyed KAP/VR. The difference between the bulk and single-molecule results may be attributed to insufficient sampling and/or concentration-dependent growth mechanisms observed in other dyed KAP crystals.[39] Ultimately, at single-molecule doping levels, a distribution of emissive species that is well-modeled by two Gaussian subpopulations with maxima shifted from the ensemble maximum by ~10 and ~30 nm is observed.

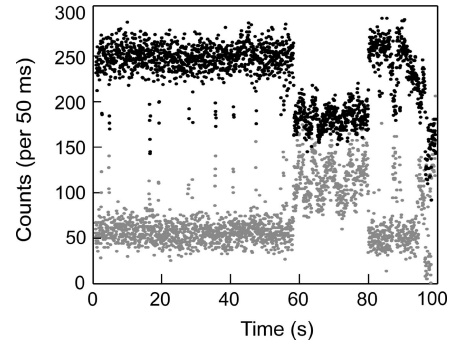

Figure 5. Representative emission time trace separated into reflected (black, >600 nm) and transmitted (gray, 550−600 nm) intensities where anticorrelation is indicative of spectral diffusion. Periods of anticorrelation between 0.05 and 60 s, correlation between 60 and 80 s, and recovered anticorrelation >80 s are demonstrated.

To determine if single molecules exhibit spectral diffusion, the reflected and transmitted intensities were measured as a function of time. A representative single-molecule emission time trace wherein the emission is separated onto reflected and transmitted detectors is presented in Figure 5. For this particular molecule, the reflected and transmitted intensities exhibit periods of anticorrelation (e.g., from 0.05 to ~60 s) and correlation (e.g., ~60 to ~80 s). Anticorrelation is consistent with spectral diffusion, that is, fluctuations in the emission energy across the dichroic mirror. However, the molecule also demonstrates intensity fluctuations when the emission intensity is correlated, suggesting that intensity fluctuations arise from both spectral diffusion and another mechanism that modifies the transition dipole moment (e.g., conformational flexibility).[13,21] No correlations were detected between the emission intensity and temporal duration of the blinking events.

One prediction of the spectral-diffusion model is that assuming a constant Stokes shift between the absorption and fluorescence band, the measured spectral fluctuations of the emission spectrum must be accompanied by a shift in the absorption spectrum. A shift of the molecular absorption spectrum will modify the absorption cross-section of the molecule, leading to fluctuations in emissive intensity.[12,21,22,37,40,41] Applying this prediction to KAP/VR, one expects that substantially red-shifted emission will correspond to low-intensity emissive periods since the absorption cross section of VR will be reduced. For example, considering the Stokes shift of heavily dyed KAP/VR is 64 nm, an average ΔE of -760 cm^{-1} corresponds to emission and absorption energies of 15 659 (639) and 17 391 cm^{-1} (575 nm), respectively, and a reduction to the absorption cross section by ~80% ($\sigma_{\mathrm{KAP/VR\ (aq)}}(575\ \mathrm{nm}) = 7030\ \mathrm{M^{-1}\ cm^{-1}}$) relative to absorption at 532 nm ($\sigma_{\mathrm{KAP/VR\ (aq)}}(532\ \mathrm{nm}) = 37\,500\ \mathrm{M^{-1}\ cm^{-1}}$). Therefore, these red-shifted emission events should be ~80% less intense than the ensemble-averaged (i.e., most probable) emission events. To explore the relationship between emission energy and intensity, average ΔE was plotted as a function of normalized intensity (Figure 6). The data in Figure 6 demonstrates that the most red-shifted emission corresponds to the brightest intensity, inconsistent with spectral diffusion. Yet, the Stokes shift may be dependent upon the local dielectric environment. Therefore, our data is consistent with one of two hypotheses: (1) distributed kinetics from single VR molecules in KAP are attributed to spectral diffusion, wherein a dye

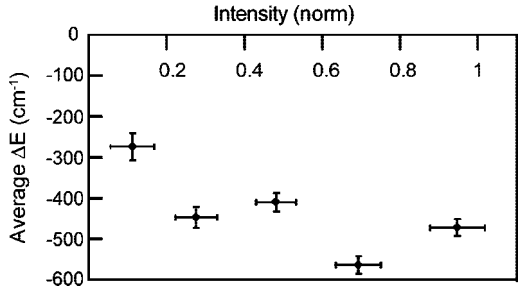

Figure 6. Plot of average ΔE versus normalized intensity for 61 molecules of VR in KAP with error bars corresponding to the standard deviation of the mean. Spectral diffusion would be manifest as a reduction in emission intensity as the energy is substantially shifted from the ensemble-averaged value. In contrast, the data demonstrates that the most red-shifted emission is the brightest.

experiences time-dependent changes to the surrounding dielectric that modify its Stokes shift and emission intensity, or (2) spectral diffusion occurs in KAP/VR but may only serve to promote the population and depopulation of a nonemissive state.

Role of Electron Transfer in Distributed Kinetics. Power-law blinking behavior of single molecules has been attributed to charge separation and recombination events corresponding to diffusion-controlled electron transfer,[34,42–44] photoinduced spectral diffusion of donor and acceptor levels, [34] and electron or hole tunneling.[6,8,28,31,33] The diffusion-controlled electron transfer model (DCET)[43,44] involves charge ejection from the excited-state and distributed recombination rates that are a consequence of the disordered surroundings.[42] Although power-law behavior for the off times is predicted by DCET, single-exponential statistics are expected for the on times, consistent with a single rate for charge separation from the excited state. Thus, the DCET model cannot account for universal power-law behavior (i.e., both on and off times being power-law distributed). The photoinduced spectral diffusion model involves one-dimensional diffusion in energy space of donor and acceptor energy levels[45] and predicts power-law exponents of 1.5.[34,46] Finally, power-law statistics for the on and off times for single molecules of rhodamine 6G in poly(vinyl alcohol),[16] and on glass,[10] perylene diimide molecules in PMMA,[6] as well as Atto565 on glass[14] have been assigned to the formation of nonemissive radicals by electron tunneling with power-law exponents ranging between 1 and 2. In these systems, the dynamic and heterogeneous environment that surrounds the molecule is thought to be responsible for an exponential distance-dependence of tunneling rates.[8] Support for electron tunneling was provided by Zondervan et al., who measured a weak temperature dependence of the lifetime of the dark state as well as the ESR spectrum of a photoexcited polymer film containing single molecules of rhodamine 6G and observed a transition consistent with radical formation.[16]

In contrast to previous studies on glass or in polymers, we observed distributed kinetics for molecules incorporated in a rigid, ordered, and well-defined crystalline environment.[13] Applying the CPD method to the blinking dynamics in KAP/VR revealed power-law exponents of ~1.5, consistent with electron tunneling and photoinduced spectral diffusion of electron donor and acceptor energy levels. Akin to mechanisms proposed for single molecules on glass and in polymers,[14,16] it is possible that VR undergoes intermolecular electron transfer to/from the KAP crystal. For example, it is known that during growth from solution cationic impurities are introduced into the KAP lattice (e.g., Fe^{3+}).[47] These cationic defects are holes that can accept electrons from the electron-rich VR chromophore. Consequently, distributed kinetics could arise from the disordered spatial distribution of holes or spectral diffusion of electron donor levels. Both models are consistent with our spectral-diffusion experiments that demonstrated that the local environments in KAP are diverse and may vary with time. In order to differentiate between these mechanisms, temperature-dependent blinking studies will be performed, since electron tunneling should demonstrate weak temperature dependence while photoinduced spectral diffusion is strongly dependent on thermal energy.

Memory in Single-Molecule Emission. To gain more insight into the origin of distributed kinetics in quantum dots, previous studies examined the correlations between adjacent on and off times.[28,29,48] The idea behind these studies was that the presence or absence of correlations would provide information on the time scale for dielectric fluctuations affecting the rate of dark-state population and depopulation. If changes to the rate constants governing the population and depopulation of the dark state are slower than the blinking rate, then adjacent emissive and nonemissive events should be correlated. This correlation is called "memory". On the other hand, if the fluctuations are fast compared to the blinking rate, the temporal duration of adjacent emissive/nonemissive events will not be correlated. Stefani et al. demonstrated that memory is indeed observed for ZnCdSe quantum dots, suggesting that the fluctuations occur more slowly than the blinking time scale.[29] In contrast, studies by Nesbitt and co-workers found no correlation in the emission from InP and CdSe quantum dots, but power-law behavior was still observed.[28,48] This observation suggests that fluctuations in the rate constants for dark-state population and depopulation occur on the blinking time scale, consistent with charge ejection changing the local environment thereby erasing any memory between successive blinking events. The relationship between power-law behavior and the presence (or absence) of memory effects in the blinking dynamics of semiconductor quantum dots has yet to be definitively established.

Correlations between adjacent on and off times in the blinking dynamics of single VR molecules in KAP were examined by analyzing $x-y$ plots on logarithmic scales consistent with previous studies.[29] First, the blinking dynamics of 40 molecules in KAP/VR were compiled to produce plots of the temporal durations of successive emissive and nonemissive events as shown in Figure 7A. The linear Pearson correlation coefficient (R_{log}) was used to quantify correlations between adjacent times. The limiting values of R_{log} are 1 and -1 corresponding to positive and negative correlation, respectively, and R_{log} values close to zero indicate no correlation. Therefore, deviations from zero suggest correlations, and are visually manifested as an enhancement of point density along the diagonal ($x = y$) in the scatter plots. The greater point density along the diagonal for plots of consecutive on times (Figure 7A, a) and off times (Figure 7A, b) demonstrates the existence of memory for VR in KAP. Consistent with this observation, adjacent on times and adjacent off times exhibit positive correlations with R_{log} values of 0.48 and 0.50, respectively. In contrast, the plot of consecutive on and off times (Figure 7A, c) demonstrates a paucity of points along the diagonal, consistent with anticorrelation of successive on and off events. Quantitatively, consecutive on and off times exhibit a weak negative correlation ($R_{log} = -0.12$) consistent with anticorrelation.

Previously we demonstrated that individual VR molecules demonstrate power-law blinking behavior, an observation that highlights the photochemical stability provided by the KAP lattice.[49,50] In order to establish that individual molecules exhibit

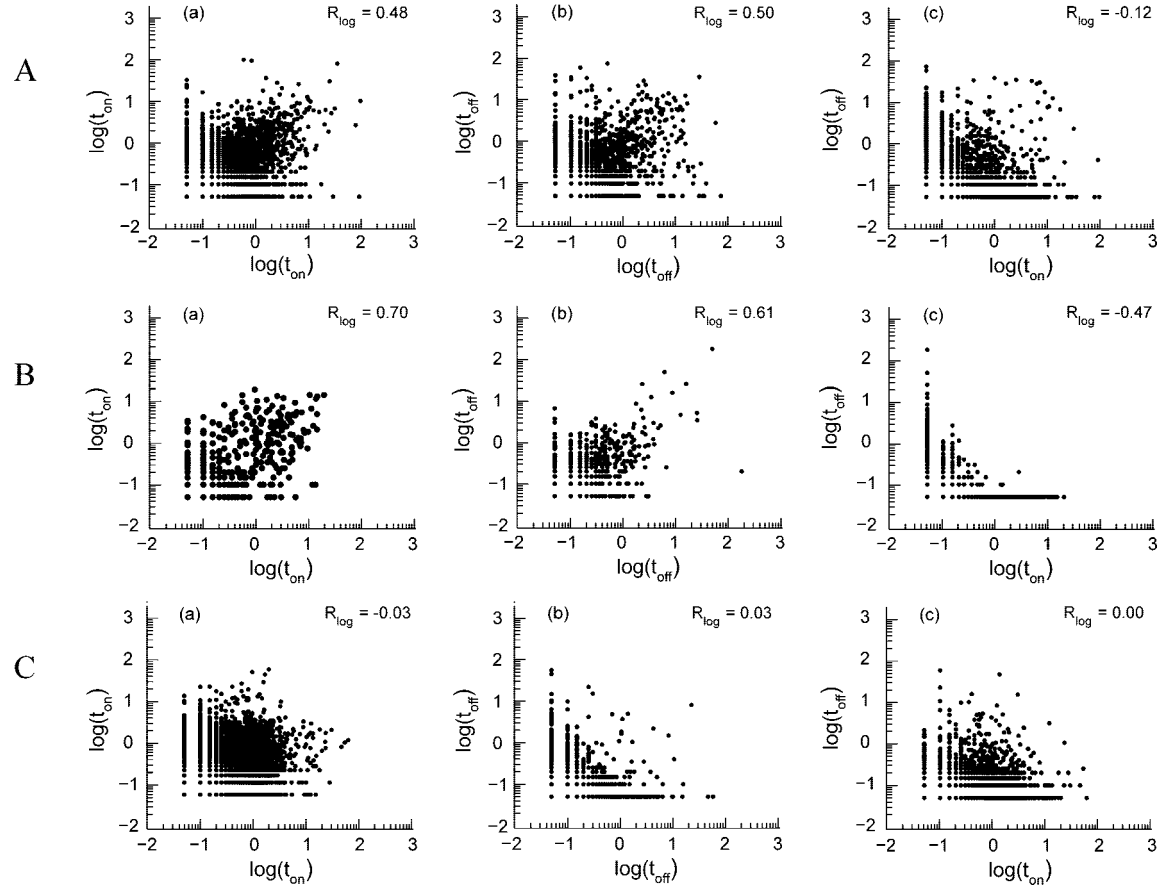

Figure 7. A. Correlations of adjacent on and off times (in seconds) obtained from 40 molecules of VR in KAP. B. Correlations of adjacent on and off times obtained from an individual molecule of VR in KAP. C. Correlations of adjacent on and off times obtained from 40 Monte Carlo simulations. Scatter plots of (a) on times (t_{on} vs t_{on}), (b) off times (t_{off} vs t_{off}), and (c) on and off times (t_{on} vs t_{off}) are presented on logarithmic scales with corresponding correlation coefficients (R_{log}).

memory, and that the correlations evident in Figure 7 do not arise from sampling over many populations, we performed a similar correlation analysis on the emission observed from individual molecules. All molecules that exhibited blinking for >1000 s (long enough to provide sufficient statistics) produced power-law behavior and nonzero correlation coefficients, with $\langle R_{log,on}\rangle = 0.26 \pm 0.23$, $\langle R_{log,off}\rangle = 0.45 \pm 0.24$, and $\langle R_{log,on/off}\rangle = -0.21 \pm 0.18$, consistent with the coefficients observed for the collection of molecules. Representative correlation plots of adjacent on and off times for a single molecule of KAP/VR are presented in Figure 7B. In agreement with the ensemble correlations, the molecule exhibits positive correlations for consecutive on times ($R_{log} = 0.70$) and consecutive off times ($R_{log} = 0.61$) as well as anticorrelated on and off times ($R_{log} = -0.47$). To our knowledge, this is the first reported observation of memory for an individual molecular system. That memory has not been previously reported for molecular systems is likely due to the advent of photobleaching that limits the statistics that can be acquired on a single molecule. However, when incorporated into KAP, single fluorophores can exhibit emission for thousands of seconds.[13] With this advantage, we are able to study the blinking dynamics of VR over a time range that provides a sufficient statistical sample of emissive/nonemissive events allowing for the observation of memory.

In order to ensure that the observed memory effects are not artifacts of threshold selection or data analysis, we performed Monte Carlo simulations employing our previously described distributed-kinetics model,[13] subjected the simulated emission data to the analysis presented above, and investigated the resulting on- and off-time correlations. In the simulations, distributed kinetics were modeled by the random selection of a new value for x at each computational step according to $k_{ij} = \kappa_{ij}e^{-x}$. The stochastic nature of the simulations should render the resulting blinking dynamics memoryless. Figure 7C presents $x-y$ plots of adjacent on and off times from 40 Monte Carlo simulations of KAP/VR blinking dynamics. Indeed, no correlations are evident in the plots and the correlation coefficients are very close to zero. These results validate that the memory effect observed for VR in KAP do not result from threshold selection or the data analysis employed. Moreover, positive correlations were observed in adjacent on and off times from VR molecules analyzed with the CPD method, however the resulting data set was too limited for statistical treatment.

What can be learned from the observation of memory in KAP/VR? Primarily, this study provides the first evidence that the blinking dynamics of single molecules can be correlated. Memory between consecutive on and off times in the emission of single VR molecules in KAP indicates that the time scale for fluctuations in the population and depopulation kinetics of the nonemissive state are slower than the typical blinking rate. We previously measured the average blinking rate for KAP/VR to be 1.37 ± 1.94 s^{-1};[13] therefore, fluctuations in k_{ij} must occur on a relatively shorter time scale. The correlations also provide information about the nature of the dark state. Current working hypotheses for distributed kinetics in KAP/VR include spectral diffusion, electron tunneling, and photoinduced spectral diffusion of electron donor and acceptor energy levels. Spectral diffusion is based on time-dependent changes in the configu-

ration of VR relative to its local environment. The observation of an anticorrelation between consecutive on and off times is consistent with this hypothesis, since the state energies are thought to fluctuate in concert with changing guest−host interactions. That is, when the nonemissive state is closer in energy to the ground-state relative to the first excited state, the nonemissive state will be populated slowly (small k_{ij}) and then decay rapidly to the ground state (large k_{ij}). Therefore, the observation of anticorrelation of adjacent on and off events is evidence for spectral diffusion or electron transfer that occurs by distributed kinetics due to spectral diffusion of donor and acceptor energies.

Conclusion

The blinking dynamics of single VR molecules embedded in KAP were analyzed using thresholding and the change-point detection (CPD) method.[26] Data analysis employing thresholding resulted in power-law distributions of on and off times corresponding to $m \sim 2$ where only molecules that appeared to exhibit two-state blinking were considered. When the same emission time traces were analyzed with the CPD algorithm, power-law behavior was modified from $m \sim 2$ to $\sim$1.5, consistent with a reduction in short time events, a consequence of the inclusion of statistically insignificant events associated with Poisson-distributed counting noise and shot noise. Moreover, multiple emission states were observed from molecules of VR in KAP, inconsistent with a simple two-state blinking model. These results demonstrate that the CPD method should be used for proper analysis of single-molecule blinking dynamics, particularly for experiments employing short bin times (that lead to small signal-to-noise), as are planned.

In our previous analysis, we demonstrated that the power-law behavior ($m \sim 2$) in KAP/VR was consistent with a distributed-kinetics model for population and depopulation of a nonemissive state.[13] It was proposed that distributed kinetics resulted from spectral diffusion and/or intermolecular charge transfer. Here, we examined the role of spectral diffusion in the distributed blinking kinetics of KAP/VR by separating two spectral components of the emission using a dichroic mirror. Combining the CPD method with this experiment yielded the emission energy, intensity, and temporal duration of blinking events. For 61 molecules in KAP/VR grown from single-molecule doping levels, a wide distribution of red-shifted emission energies were observed corresponding to two subpopulations centered at 620 and 639 nm. The wide distribution of emission energies is consistent with molecules experiencing a variety of dielectric environments within the crystal host. Time-dependent fluctuations in $R(t)$ were demonstrated, consistent with spectral diffusion. However, the most substantially red-shifted emission was found to be brightest, inconsistent with spectral diffusion as the origin for distributed kinetics if the Stokes shift remains constant. Therefore, our results support one of two hypotheses: (1) spectral diffusion occurs but it is not primarily responsible for population of a nonemissive state or (2) spectral diffusion is responsible for both emissive and nonemissive events if the Stokes shift of VR molecules changes with environment and time. To explore the latter, single-molecule experiments on KAP/VR employing various excitation energies are planned. Ultimately, evidence for spectral diffusion is demonstrated, consistent with the observation of multiple emissive intensities, but the role of spectral diffusion in blinking (i.e., population/depopulation of a nonemissive state) remains unclear.

Another mechanism to explain distributed kinetics in KAP/VR is intermolecular electron transfer. The observation of power-law exponents close to 1.5 is consistent with electron tunneling and photoinduced spectral diffusion of electron donor and acceptor energy levels. For example, trivalent cationic impurities introduced into the KAP lattice during crystal growth can accept electrons from the electron-rich VR chromophore. In this example, distributed kinetics could be a consequence of a disordered spatial distribution of holes or spectral diffusion of electron donor energy levels. To differentiate between these possibilities, experiments to explore the temperature dependence of blinking dynamics are planned. In view of the observations of spectral diffusion and a broad distribution of emission energies, we propose that blinking in KAP/VR is related to photoinduced spectral diffusion of electron donor and acceptor levels. This hypothesis is supported by the observation of memory in the emission from single molecules in KAP/VR as well as an anticorrelation between adjacent on and off events.

Finally, our results from implementation of the CPD method, measurements of single-molecule spectral diffusion and memory demonstrate the need to perform blinking experiments in more well-defined local environments. Specifically, our previous single-molecule studies of orientation[25] and photophysics[13] along with the results presented here demonstrate a significant amount of environmental heterogeneity in dyed KAP crystals. Consequently, blinking studies on dyed crystals that exhibit narrow orientational distributions (i.e., basic pyranine in K_2SO_4)[25] where environmental heterogeneity is reduced will be performed.

Acknowledgment. We thank the National Science Foundation for the generous support of this work through the Center on Materials and Devices for Information Technology Research (DMR-0120967). K.L.W. is a NSF-IGERT and University Initiative Funded fellow, supported by the Center for Nanotechnology at the University of Washington (DGE-0504573). B.K. acknowledges NSF Grant CHE-0349882. We thank Haw Yang for helpful discussions about the change-point detection algorithm.

References and Notes

(1) Basche, T.; Kummer, S.; Brauchle, C. *Nature* **1995**, *373*, 132.
(2) Kohn, F.; Hofkens, J.; Gronheid, R.; Van der Auweraer, M.; De Schryver, F. C. *J. Phys. Chem. A* **2002**, *106*, 4808.
(3) Veerman, J. A.; Garcia-Parajo, M. F.; Kuipers, L.; van Hulst, N. F. *Phys. Rev. Lett.* **1999**, *83*, 2155.
(4) Kulzer, F.; Kummer, S.; Basche, T.; Brauchle, C. *J. Inf. Rec.* **1996**, *22*, 567.
(5) Haase, M.; Hubner, C. G.; Reuther, E.; Herrmann, A.; Mullen, K.; Basche, T. *J. Phys. Chem. B.* **2004**, *108*, 10445.
(6) Hoogenboom, J. P.; Hernando, J.; van Dijk, E.; van Hulst, N. F.; Garcia-Parajo, M. F. *Chem. Phys. Chem.* **2007**, *8*, 823.
(7) Hoogenboom, J. P.; van Dijk, E.; Hernando, J.; van Hulst, N. F.; Garcia-Parajo, M. F. *Phys. Rev. Lett.* **2005**, *95*, 097401.
(8) Kuno, M.; Fromm, D. P.; Johnson, S. T.; Gallagher, A.; Nesbitt, D. J. *Phys. Rev. B* **2003**, *67*, 125304.
(9) Osad'ko, I. S. *J. Exp. Theor. Phys.* **2003**, *96*, 617.
(10) Schuster, J.; Cichos, F.; von Borczyskowski, C. *Opt. Spectrosc.* **2005**, *98*, 712.
(11) Schuster, J.; Cichos, F.; von Borczyskowski, C. *Appl. Phys. Lett.* **2005**, *87*, 051915.
(12) Weston, K. D.; Buratto, S. K. *J. Phys. Chem. A* **1998**, *102*, 3635.
(13) Wustholz, K. L.; Bott, E. D.; Isborn, C. M.; Li, X.; Kahr, B.; Reid, P. J. *J. Phys. Chem. C* **2007**, *111*, 9146.
(14) Yeow, E. K. L.; Melnikov, S. M.; Bell, T. D. M.; De Schryver, F. C.; Hofkens, J. *J. Phys. Chem. A* **2006**, *110*, 1726.
(15) Yip, W. T.; Hu, D. H.; Yu, J.; Vanden Bout, D. A.; Barbara, P. F. *J. Phys. Chem. A* **1998**, *102*, 7564.
(16) Zondervan, R.; Kulzer, F.; Orlinskii, S. B.; Orrit, M. *J. Phys. Chem. A* **2003**, *107*, 6770.
(17) Clifford, J. N.; Bell, T. D. M.; Tinnefeld, P.; Heilemann, M.; Melnikov, S. M.; Hotta, J. i.; Sliwa, M.; Dedecker, P.; Sauer, M.; Hofkens, J.; Yeow, E. K. L. *J. Phys. Chem. B* **2007**, *111*, 6987.
(18) Ambrose, W. P.; Goodwin, P. M.; Martin, J. C.; Keller, R. A. *Phys. Rev. Lett.* **1994**, *72*, 160.

(19) Ambrose, W. P.; Basche, T.; Moerner, W. E. *J. Chem. Phys.* **1991**, *95*, 7150.
(20) Lu, H. P.; Xie, X. S. *Nature* **1997**, *385*, 143.
(21) Stracke, F.; Blum, C.; Becker, S.; Mullen, K.; Meixner, A. J. *ChemPhysChem* **2005**, *6*, 1242.
(22) Stracke, F.; Blum, C.; Becker, S.; Mullen, K.; Meixner, A. J. *Chem. Phys.* **2004**, *300*, 153.
(23) Christ, T.; Kulzer, F.; Bordat, P.; Basche, T. *Angew. Chem., Int. Ed. Engl.* **2001**, *40*, 4192.
(24) Yu, J.; Hu, D. H.; Barbara, P. F. *Science* **2000**, *289*, 1327.
(25) Wustholz, K. L.; Kahr, B.; Reid, P. J. *J. Phys. Chem. B* **2005**, *109*, 16357.
(26) Watkins, L. P.; Yang, H. *J. Phys. Chem. B* **2005**, *109*, 617.
(27) Zhang, K.; Chang, H. Y.; Fu, A. H.; Alivisatos, A. P.; Yang, H. *Nano Lett.* **2006**, *6*, 843.
(28) Kuno, M.; Fromm, D. P.; Hamann, H. F.; Gallagher, A.; Nesbitt, D. J. *J. Chem. Phys.* **2001**, *115*, 1028.
(29) Stefani, F. D.; Zhong, X. H.; Knoll, W.; Han, M. Y.; Kreiter, M. *New J. Phys.* **2005**, *7*, 197.
(30) Hoogenboom, J. P.; den Otter, W. K.; Offerhaus, H. L. *J. Chem. Phys.* **2006**, *125*, 204713.
(31) Verberk, R.; van Oijen, A. M.; Orrit, M. *Phys. Rev. B* **2002**, *66*, 233202.
(32) Stefani, F. D.; Knoll, W.; Kreiter, M.; Zhong, X.; Han, M. Y. *Phys. Rev. B* **2005**, *72*, 125304.
(33) Issac, A.; von Borczyskowski, C.; Cichos, F. *Phys. Rev. B* **2005**, *71*, 161302.
(34) Tang, J.; Marcus, R. A. *J. Chin. Chem. Soc.* **2006**, *53*, 1.
(35) English, D. S.; Harbron, E. J.; Barbara, P. F. *J. Chem. Phys.* **2001**, *114*, 10479.
(36) Bardoux, R.; Guillet, T.; Lefebvre, P.; Taliercio, T.; Bretagnon, T.; Rousset, S.; Gil, B.; Semond, F. *Phys. Rev. B* **2006**, *74*, 195319.
(37) Ha, T.; Enderle, T.; Chemla, D. S.; Selvin, P. R.; Weiss, S. *Phys. Rev. Lett.* **1996**, *77*, 3979.
(38) Jung, C.; Hellriegel, C.; Platschek, B.; Wohrle, D.; Bein, T.; Michaelis, J.; Brauchle, C. *J. Am. Chem. Soc.* **2007**, *129*, 5570.
(39) Bullard, T.; Wustholz, K. L.; Robertson, M.; Reid, P. J.; Kahr, B. Unpublished results.
(40) Weston, K. D.; Goldner, L. S. *J. Phys. Chem. B* **2001**, *105*, 3453.
(41) Xie, X. S.; Dunn, R. C. *Science* **1994**, *265*, 361.
(42) Margolin, G.; Barkai, E. *J. Chem. Phys.* **2004**, *121*, 1566.
(43) Tang, J.; Marcus, R. A. *Phys. Rev. Lett.* **2005**, *95*, 107401.
(44) Tang, J.; Marcus, R. A. *J. Chem. Phys.* **2005**, *123*, 204511.
(45) Empedocles, S. A.; Bawendi, M. G. *J. Phys. Chem. B* **1999**, *103*, 1826.
(46) Bouchaud, J. P.; Georges, A. *Phys. Rep.* **1990**, *195*, 127.
(47) Hottenhuis, M. H. J.; Oudenampsen, A. *J. Cryst. Growth* **1988**, *92*, 513.
(48) Kuno, M.; Fromm, D. P.; Gallagher, A.; Nesbitt, D. J.; Micic, O. I.; Nozik, A. J. *Nano Lett.* **2001**, *1*, 557.
(49) Benedict, J. R.; Wallace, P. M.; Reid, P. J.; Jang, S. H.; Kahr, B. *Adv. Mater.* **2003**, *15*, 1068.
(50) Rifani, M.; Yin, Y. Y.; Elliott, D. S.; Jay, M. J.; Jang, S. H.; Kelley, M. P.; Bastin, L. D.; Kahr, B. *J. Am. Chem. Soc.* **1995**, *117*, 7572.

JP711687J